

***In vitro* Activity of Picroside I in Type 2 Diabetes Based on Oxidative Stress**

Jingya Liu^a, Yinqiu Zheng^a, Shuang Dai, Li Li, Wei Wu, Rong Gou, Deyuan Wang, Shiyu Long, Meihua Huang, Zhihong Xu*

School of Science, Xihua University, Chengdu, 610039, China.

*Corresponding author: Zhihong Xu, email: xuzh@mail.xhu.edu.cn; Phone: +86 13666265456.

^aThese authors contributed equally: Jingya Liu and Yinqiu Zheng.

Received November 3rd, 2022; Accepted February 24th, 2023.

DOI: <http://dx.doi.org/10.29356/jmcs.v67i2.1899>

Abstract. The primary factor leading to insulin resistance (IR) and type 2 diabetes mellitus (T2DM) is oxidative stress. Despite its liver-protecting, enzyme-lowering, immune-regulating, and antiviral effects, the impact of picroside I on oxidative stress, glucose utilization, and IR has not been investigated yet. *In vitro* studies were conducted to evaluate the antioxidant properties of different concentrations of picroside I. The results showed that picroside I effectively suppresses α -glucosidase and α -amylase with IC_{50} values of 109.75 μ g/mL and 160.71 μ g/mL in the range of 50-500 μ g/mL. Additionally, when IR-HepG2 cells were treated with 80 μ g/mL of picroside I, it was found to have little effect on cell viability, increase glucose consumption, decrease the levels of the free radical metabolite malonic dialdehyde, and increase superoxide dismutase activity. These findings indicate that picroside I has the potential to regulate oxidative stress in IR-HepG2 cells, potentially improving IR and exhibiting anti-T2DM activity.

Keywords: Picroside I; oxidative stress; insulin resistance (IR); glucose consumption; HepG2 cells.

Resumen. El factor principal que conduce a la resistencia a la insulina (IR) y a la diabetes mellitus tipo 2 (T2DM) es el estrés oxidativo. A pesar de sus efectos protectores del hígado, reductores de enzimas, inmunorreguladores y antivirales, aún no se ha investigado el impacto del picróside I sobre el estrés oxidativo, la utilización de glucosa y la IR. Se realizaron estudios *in vitro* para evaluar las propiedades antioxidantes de diferentes concentraciones de picróside I. Los resultados mostraron que el picróside I suprime eficazmente la α -glucosidasa y la α -amilasa con valores IC_{50} de 109,75 μ g/mL y 160,71 μ g/mL en el rango de 50 -500 microgramos/ml. Además, cuando las células IR-HepG2 se trataron con 80 μ g/mL de picróside I, se encontró que tenía poco efecto sobre la viabilidad celular, aumentaba el consumo de glucosa, disminuía los niveles del metabolito de radicales libres dialdehído malónico y aumentaba la actividad de la superóxido dismutasa. Estos hallazgos indican que el picróside I tiene el potencial de regular el estrés oxidativo en las células IR-HepG2, mejorando potencialmente la IR y exhibiendo actividad anti-T2DM.

Palabras clave: Picróside I; estrés oxidativo; resistencia a la insulina (RI); consumo de glucosa; células HepG2.

Introduction

T2DM is a metabolic disorder defined by elevated blood glucose levels and decreased function of the β -cells in the pancreas. This condition arises from a combination of genetic and environmental factors, insulin resistance, and inadequate insulin secretion [1-4].

Oxidative stress refers to an excessive accumulation of reactive oxygen species (ROS) in the body, which results in an imbalance between oxidation and protection. This leads to tissue, cell, and biological molecule damage, such as to nucleic acids and proteins [5,6]. ROS, including superoxide anions, oxygen radicals, hydrogen peroxide, and lipid peroxide, are powerful oxidants generated in eukaryotic cells through normal metabolism. The lipid peroxidation of biofilm-bound unsaturated fatty acids results in the formation of malonic dialdehyde (MDA), conjugated diene, and 4-hydroxynonenal [7]. Among these, MDA can combine and cross-link with proteins and enzymes on the cell membrane, altering its fluidity and permeability and impacting physiological and biochemical reactions. Therefore, MDA serves as an indicator of lipid peroxidation and oxidative cell damage [8]. The presence of elevated free radicals can worsen diabetes [9,10]. The body's defense against oxidative damage is aided by the enzyme superoxide dismutase (SOD), which can neutralize superoxide anions and protect cells [11-14]. The SOD activity level reflects the body's capacity to remove oxygen-free radicals, while the MDA content can be used to gauge the extent of free radical attack on cells.

Oxidative stress plays a central role in the development of insulin resistance (IR), which is the underlying cause of T2DM [15-20]. Therefore, addressing IR is crucial in treating T2DM. The treatment of T2DM can be approached in two ways. The first is to limit the source of glucose in the blood by reducing sugar intake, decreasing insulin breakdown into muscle and liver glycogen, and converting non-sugar substances into glucose. The second is to promote the conversion of glucose in the blood into non-sugar substances and glycogen, thereby lowering blood glucose levels. For centuries, plant-based medicines have been used to treat diabetes [21], especially in developing countries.

Picroside I, an iridoid glycoside extracted from the picrorhiza rhizome, has been shown to have cholagogue effects, improve liver function, protect against liver injury caused by free radical release, enhance antioxidant enzyme activity, and support liver health [22]. However, its potential for treating T2DM is unknown. This study aimed to evaluate the *in vitro* antioxidant properties of picroside I and to examine its impact on insulin resistance in human hepatocellular carcinoma (HepG2) cells, in order to explore its potential as an anti-T2DM drug based on its effect on oxidative stress.

Experimental

Material and methods

Materials

Picroside I and vitamin C were supplied by Chengdu Desite Biotechnology Incorporation. α -Amylase, α -glucosidase, acarbose, recombinant human insulin, rosiglitazone, glucose oxidase (GOD) activity assay kit, SOD assay kits, and MDA assay kits were provided by Beijing Solarbio Technology Co., Ltd. All other reagents were from Chengdu Cologne Chemical Co., Ltd.

In vitro antioxidant activity assays of compounds

2, 2-Diphenyl-1-picrylhydrazyl radical (DPPH•) scavenging activity assay

DPPH• scavenging activity was used to evaluate the scavenging activity of the compounds against free radicals and measured according to a previously described approach [23], with some modifications. In the experimental group, 100 μ L of picroside I (10, 20, 30, 40, 50 μ g/mL) and 100 μ L of DPPH• (0.2 M) were added to the 96-well plates. In the negative control group, 100 μ L of ethanol absolute was substituted for picroside I. In the blank control group, 100 μ L of ethanol absolute was used instead of DPPH• (0.2 M). After standing in the dark for 30 min at room temperature (RT), the absorbance of all wells was determined at 517 nm.

Vitamin C (10, 20, 30, 40, 50 µg/mL) was applied as the positive control, and all groups were assayed in triplicate to evaluate the scavenging activity.

$$\text{DPPH} \bullet \text{ scavenging activity}(\%) = \left(1 - \frac{A_S - A_0}{A_N}\right) \times 100\% \quad (1)$$

where A_S , A_N , and A_0 represent the absorbance of the experimental group, the negative control group, and the blank control group, respectively. The physical quantities represented by the same parameters in the following formulas are consistent with formula (1).

2,2'-Azino-bis-(3-ethylbenzothiazoline-6-sulfonate) radical (ABTS^{•+}) scavenging activity assay

ABTS^{•+} scavenging activity was used to evaluate the scavenging activity of compounds against free radicals, and it was measured based on a previously described approach [24] with slight modifications. At first, 7.4 mM ABTS^{•+} solution was blended with 2.6 mM K₂S₂O₄ solution at a volume ratio of 1:1 to prepare ABTS^{•+} stock solution. The stock solution was stored in a refrigerator and left overnight, then, diluted 20 times with ethanol absolute as ABTS^{•+} working solution. In the experimental group, 50 µL of picroside I (10, 20, 30, 40, 50 µg/mL) and 200 µL of ABTS^{•+} working solution were blended. In the negative control group, picroside I was replaced with 50 µL of ethanol absolute. In the blank control group, ABTS^{•+} working solution was used instead of 200 µL of ethanol absolute. After standing for 10 min in the dark at RT, the absorbance was determined at 734 nm. Vitamin C (10, 20, 30, 40, 50 µg/mL) was employed as the positive control, and all groups were assayed in triplicate.

$$\text{ABTS} \bullet^+ \text{ scavenging activity}(\%) = \left(1 - \frac{A_S - A_0}{A_N}\right) \times 100\% \quad (2)$$

Hydroxyl radical scavenging activity assay

Hydroxyl radical-scavenging activity was determined based on a previously described approach [25], with some modifications. 50 µL of picroside I (50, 100, 200, 300, 400, 500 µg/mL), 50 µL of FeSO₄ (9 mM), and 50 µL of salicylic acid (9 mM) were added to 96-well plates. Then, 50 µL of H₂O₂ (0.1 %) solution was mixed with the solution and cultured for 60 min at 37 °C. In the blank group, an equivalent volume of deionized water was used instead of the H₂O₂ solution. An equivalent volume of ethanol absolute was substituted for picroside I in the negative control group. Vitamin C (50, 100, 200, 300, 400, 500 µg/mL) was applied as a positive control. All groups were assayed three times. The absorbance was determined at 510 nm. Hydroxyl radical scavenging activity was calculated as follows:

$$\text{Hydroxyl radical scavenging activity}/\% = \left(1 - \frac{A_S - A_0}{A_N}\right) \times 100\% \quad (3)$$

Reduction ability

The reducibility of compounds was accurately measured using a previously described approach [26] with some modifications. About 300 µL of a solution containing various contents of picroside I (2.5, 5, 10, 15, 20, 25 µg/mL), 300 µL of phosphate-buffered saline (PBS, 0.2 M, pH=6.6), and 300 µL of K₃Fe(CN)₆ (1 %) were reacted in water for 20 minutes at 50 °C. After cooling, 300 µL of trichloroacetic acid (10 %) was added to compound solutions, mixed, and centrifuged for 10 min at 3000 r/min. About 300 µL of supernatant, 300 µL of distilled water, and 75 µL of FeCl₃ (0.1 %) were mixed. Then, 200 µL of reaction solutions were added to the 96-well plates and allowed to stand for 10 min. The absorbance was determined at 700 nm. In the blank control group, FeCl₃ (0.1 %) was replaced with distilled water. Vitamin C (2.5, 5, 10, 15, 20, 25 µg/mL) was employed as a positive control for evaluating the total reduction capacity. Each group was assayed in triplicate.

$$\Delta A = A_S - A_0 \quad (4)$$

Determination of α -glucosidase activity inhibition

The α -glucosidase activity of compounds was measured using a previously described approach [27] with some modifications. The specimens were prepared with PBS (100 mM, pH=6.8). 25 μ L of Picroside I (50, 100, 200, 300, 400, 500 μ g/mL) and 15 μ L of α -glucosidase (0.5 U/mL) were added into 96-well plates. After incubating for 10 min at 37 °C, 30 μ L of *p*-nitrophenol- α -D-glucopyranoside (5 mM) was added. Then, the blend was cultured for 25 min at 37 °C, and 100 μ L of Na₂CO₃ (0.2M) termination solution was added. In the blank control group, picroside I was replaced with PBS (100 mM, pH=6.8); in the negative control group (1), the α -glucosidase solution was replaced with PBS (100 mM, pH=6.8); and in the negative control group (2), picroside I and α -glucosidase solution were replaced with PBS (100 mM, pH=6.8). Then the absorbance at 405 nm was determined with the microplate reader. Acarbose (50, 100, 200, 300, 400, 500 μ g/mL) was adopted as the positive control. All groups were assayed in triplicate. The α -glucosidase suppression rate was calculated as follows:

$$\alpha - \text{glucosidase inhibition rate}(\%) = \left(1 - \frac{A_S - A_0}{A_{N_1} - A_{N_2}}\right) \times 100\% \quad (5)$$

where A_S , A_0 , A_{N_1} , and A_{N_2} represent the absorbance of the sample, blank control group, negative control group (1), and negative control group (2), respectively.

Determination of α -amylase activity inhibition

The α -amylase activity inhibition of compounds was measured based on a previously depicted approach [28] with some modifications. About 60 μ L of α -amylase (15 U/mL), 120 μ L of picroside I (50, 100, 200, 300, 400, 500 μ g/mL), and 300 μ L of PBS (20 mM, pH=6.8) were added to test tubes. The blend was pre-incubated for 10 min at 37 °C; thereafter, 120 μ L of amyllum (1 %) was added. Then, the blend was mixed and incubated for 5 min at 37 °C. The reaction was terminated with 480 μ L of DNS. The test tubes were placed in a boiling water bath for 15 min, cooled to RT, added with 1860 μ L of PBS (20 mM, pH=6.8), and diluted to an appropriate volume. In the blank control group, picroside I was replaced with PBS (20 mM, pH=6.8). In the negative control group (1), the α -amylase was replaced with PBS (20 mM, pH=6.8). In the negative control group (2), picroside I and α -amylase were replaced with PBS (20 mM, pH= 6.8). The absorbance was recorded at 540 nm with a microplate reader. Acarbose (50, 100, 200, 300, 400, 500 μ g/mL) was employed as the positive control. All groups were assayed in triplicate. The α -glucosidase suppression rate was calculated as follows:

$$\alpha - \text{glucosidase suppression rate} (\%) = \left(1 - \frac{A_S - A_0}{A_{N_1} - A_{N_2}}\right) \times 100\% \quad (6)$$

The parameters represented by each physical quantity in formula (6) are the same as those in formula (5).

Activity analysis in HepG2 cells

Cell culture

Incubating HepG2 cells were incubated in Dulbecco's Modified Eagle Medium (DMEM) supplemented with 10 % fetal bovine serum, penicillin (100 IU/mL), and streptomycin (100 μ g/mL). Cells were placed in a 37 °C, 5 % CO₂ incubator. When the cells reached 70 % - 80 % confluent at the bottom of the petri dish, the original culture medium was discarded. Thereafter, the cells were rinsed two times with PBS (pH=7.4), digested with 0.25 % trypsin, and cultured at a volume ratio of 1:2.

IR model establishment for conditional screening

MTT (3-(4,5-dimethylthiazol-2-yl)-2,5-diphenyltetrazolium bromide) was used to determine the effect of insulin action time on cell activity. The standard cultured HepG2 cells were inoculated into 96-well plates (5000 cells/well). After cell adherence (12 h), 100 μ L of DMEM containing different concentrations of insulin (10⁻⁴, 10⁻⁵, 10⁻⁶, 10⁻⁷, 10⁻⁸ M) were added in the IR model group. The blank control group was DMEM in an insulin-free

medium. Each group was cultured for 12, 24, 36, 48, and 60 h, respectively. Subsequently, 10 μL of MTT (5 mg/mL) was added to all wells and incubated for 4 h. Next, the original culture medium was discarded, and then 100 μL of DMSO was added to all wells to terminate the culture. The 96-well plates were shaken at low speed for 10 min and the absorbance was determined at 490 nm with a microplate reader. To determine the optimal time of insulin action, the cell survival rate was calculated. Each group was tested with three multiple wells.

$$\text{Cell viability(\%)} = \frac{A_S}{A_0} \times 100\% \quad (7)$$

After the optimal treatment time was determined, 100 μL of DMEM containing insulin (10^{-4} , 10^{-5} , 10^{-6} , 10^{-7} , 10^{-8} M) and glucose (25 mM) were added to the IR model group. About 100 μL of insulin-free DMEM was added to the blank group. Serum-free DMEM culture was changed after 24 h, 20 μL of supernatant was taken, and the glucose content in the culture medium was measured with a GOD activity assay kit. Glucose consumption was computed through the formula (8). The IR model group has the lowest glucose consumption rate. Each group was tested with three replicates.

$$\text{The rate of glucose consumption(\%)} = \frac{A_S}{A_0} \times 100\% \quad (8)$$

Determination of the activity of picoside I on IR-HepG2 cells

Under the established IR model, 100 μL of medium containing different concentrations of picoside I (20, 40, 80, 160, 320 $\mu\text{g/mL}$) was added and incubated in a 5 % CO_2 incubator at 37 $^\circ\text{C}$ for 24h. MTT was used to determine the effect of each concentration on IR-HepG2 cell activity, and the optimal concentration was selected as the investigational concentration. The negative control group was IR-HepG2 cells without picoside I. The culture time of each group was consistent. The absorbance of all wells was determined at 490 nm with a microplate reader. Each group was tested with three replicates. To determine the optimal concentration of drug action, the cell viability was calculated using the formula (7).

Glucose consumption of IR-HepG2 cells

After successfully establishing the best IR model, the 100 μL best content (80 $\mu\text{g/mL}$) of picoside I was added to the experimental group and incubated for 24 h. Rosiglitazone was employed as the positive control. IR-HepG2 cells without picoside I treatment were denoted as the negative control. The blank control group was not treated with insulin and picoside I. Then, the cells were cultured for another 24 h by changing the culture media into serum-free DMEM. Lastly, the GOD activity assay kit was used to detect the glucose consumption of supernatant in each group at 500 nm using a microplate reader. Each group of experiments had three replicates.

Determination of MDA content

MDA activity was determined according to the kit's instructions with slight modifications. The logarithmic growth cells were incubated into 6-well plates (500,000 cells/well). Under the condition in 2.3.2, the cells were collected in a centrifuge tube after co-incubation with the drug for 24 h. After centrifugation at RT, the supernatant was discarded. 200 μL extract of MDA activity assay kit was added, and the cells were broken using ultrasound a centrifuged at 15000 r/min and 4 $^\circ\text{C}$ for 10 min. Then, the supernatant was taken and placed on ice for testing. The determination process and reagent addition amount are shown in Table 1.

Table 1. MDA content determination and reagent addition amount

Volume (μL)	Experimental group	Negative control group
Working solution for MDA	480	480
Distilled water	0	160
Sample	160	0
Reagent III	160	160

The blend was placed in boiling water for 60 minutes and transferred to an ice bath. Then, it was centrifuged with 15,000 r/min at RT for 10 min and absorbed 200 μL supernatant into a 96-well plate. The absorbance at 450, 532, and 600 nm was measured using a microplate reader, and the absorbance was measured three times in each group. MDA content in cells was calculated as follows:

$$\Delta A_{450} = A_{450(S)} - A_{450(N)} \quad (9)$$

$$\Delta A_{532} = A_{532(S)} - A_{532(N)} \quad (10)$$

$$\Delta A_{600} = A_{600(S)} - A_{600(N)} \quad (11)$$

$$\begin{aligned} \text{The content of MDA (nmol/10}^4\text{ cell)} &= \frac{(12.9 \times (\Delta A_{532} - \Delta A_{600}) - 2.58 \times \Delta A_{450}) \times V_T \times V_E}{50 \times V_S} \quad (12) \\ &= 0.02 \times (12.9 \times (\Delta A_{532} - \Delta A_{600}) - 2.58 \times \Delta A_{450}) \end{aligned}$$

where $A_{450(S)}$, $A_{532(S)}$, and $A_{600(S)}$ represent the absorbance of cell samples at 450, 532, and 600 nm, respectively; $A_{450(N)}$, $A_{532(N)}$, and $A_{600(N)}$ represent the absorbance of the negative control group; V_T represents the total volume of the reaction system, 0.8 mL; V_E represents the extraction volume, 0.2 mL; V_S represents the volume of the sample, 0.16 mL; 50 indicates that the total number of cells is 500,000.

Determination of SOD activity

SOD activity was determined according to the kit's instructions, with slight modifications. The experimental treatment was consistent with MDA content detection. Rosiglitazone was applied as the positive control. The sample determination process and reagent addition amount are shown in Table 2.

Table 2. SOD activity determination and each reagent addition amount.

Reagent (μL)	Experimental group	Blank control group	Negative control (1)	Negative control (2)
Sample	18	18	0	0
Reagent I	45	45	45	45
Reagent II	2	0	2	0
Reagent III	35	35	35	35
Distilled water	90	92	108	110
Reagent IV	10	10	10	10

The absorbance of all wells was determined at 560 nm after the blend was bathed for 30 minutes at 37 °C. All wells were determined three times in parallel. SOD activity was computed as follows:
Calculation of suppression rate:

$$\Delta A_T = A_S - A_B \quad (13)$$

$$\Delta A_N = A_{N_1} - A_{N_2} \quad (14)$$

$$\text{Inhibition rate(\%)} = (\Delta A_N - \Delta A_T) \div \Delta A_N \times 100\% \quad (15)$$

SOD activity:

$$\text{The activity of SOD (U/10}^4\text{ cell)} = \frac{\text{Inhibition} \times V_T}{50 \times (1 - \text{Inhibition})} = \frac{0.4 \times \text{Inhibition}}{9 \times (1 - \text{Inhibition})} \quad (16)$$

In formula (13), A_S represents the absorbance of the cell specimen, and A_B refers to the absorbance of distilled water instead of reagent II. In formula (14), A_{N1} represents the absorbance of the cell sample replaced with distilled water, and A_{N2} represented the absorbance of the cell specimen and reagent II replaced with distilled water. In formula (16), V_T means the total volume of the reaction system, 0.2 mL; 50 indicates that the total number of cells is 500,000.

Data analysis

Each date in this work were calculated as average \pm standard deviation. Experiment data were processed using Origin 2017, IBM SPSS and Microsoft office 2010. The significance level was set to $p < 0.05$ to evaluate the difference of the data.

Results

Antioxidant activity *in vitro*

In the DPPH• scavenging activity assay (Fig. 1(A)), the half-maximum suppressive content (IC_{50}) of picroside I was 15.32 $\mu\text{g/mL}$. In the ABTS•⁺ scavenging activity assay (Fig. 1(B)), the IC_{50} of the compound was 12.84 $\mu\text{g/mL}$. In the hydroxyl radical scavenging activity assay (Fig. 1(C)), the IC_{50} of picroside I was 80 $\mu\text{g/mL}$. In addition, the four *in vitro* antioxidant capacity determination of DPPH• scavenging rate, ABTS•⁺ scavenging rate, hydroxyl radical scavenging rate, and reducibility (Fig. 1(D)), the antioxidant capacity rose as content rose, and the antioxidant activity of picroside I was more substantial than vitamin C. The results showed that picroside I had a high antioxidant ability.

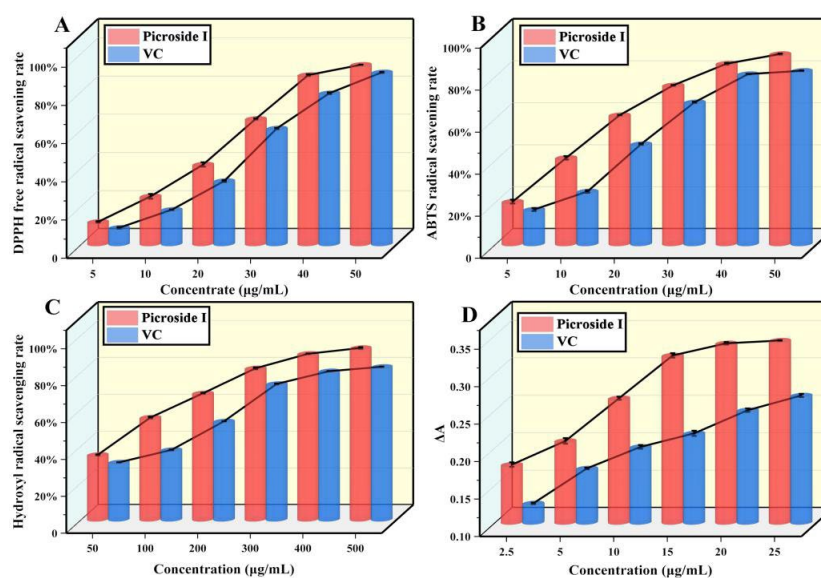


Fig 1. Determination of the antioxidant activity of picroside I *in vitro*. Determination of (A) DPPH• activity, (B) ABTS•⁺ activity, (C) hydroxyl radical activity, and (D) reducibility. ($X \pm S$, $n=6$).

Determination of α -glucosidase activity inhibition

The α -glucosidase activity inhibition was measured in the range of 50-500 $\mu\text{g/mL}$. Compared with acarbose, α -glucosidase activity inhibition was determined by IC_{50} . As shown in Fig. 2, if the content was 50-500 $\mu\text{g/mL}$, the maximum inhibition rate of picoside I on α -glucosidase was 91.67 %, and the inhibition effect of picoside I was stronger than that of acarbose. The IC_{50} of picoside I was 109.75 $\mu\text{g/mL}$. In summary, the suppression effect of picoside I on α -glucosidase was stronger than that of acarbose.

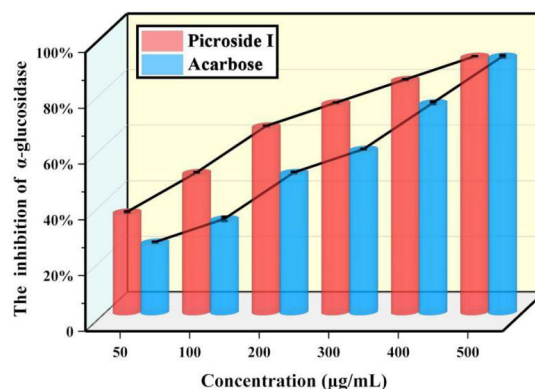


Fig 2. Suppression effect of picoside I and acarbose on α -glucosidase. ($X \pm S$, $n=6$).

Determination of α -amylase activity inhibition

Through analysis, the IC_{50} of picoside I or acarbose was obtained to measure the inhibition of compounds on α -amylase activity. The maximum suppressive rate of picoside I on α -amylase was 93.22 % (Fig. 3). The suppressive effect of picoside I on α -amylase was more potent than that of acarbose at a concentration of 50-500 $\mu\text{g/mL}$. The IC_{50} of picoside I was 160.71 $\mu\text{g/mL}$, lower than acarbose (221.81 $\mu\text{g/mL}$). In conclusion, it can be concluded that picoside I, has a more potent inhibitory effect on α -amylase than acarbose.

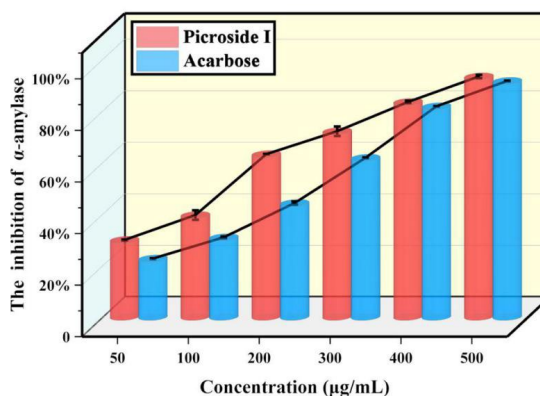


Fig 3. Inhibitory effect of picoside I and acarbose on α -amylase. ($X \pm S$, $n=6$).

Effect of insulin on HepG2 cells

As shown in Fig. 4(A), insulin inhibited HepG2 cell activity in a concentration-dependent manner except after 12 h of treatment. When treated for 36 h, the cell viability decreased significantly with increasing concentration, even below 90 % ($P < 0.05$). When the treatment time was extended to 60 h, the inhibition of insulin activity was more significant ($P < 0.05$). The low cell activity might be due to the lack of nutrients provided by the culture medium. Therefore, to exclude the effect of insulin action time on cell viability, 24 h was taken as the best investigational time of insulin.

Fig. 4(B) exhibited that after 24 h treatment with DMEM and insulin-containing 25 mM glucose, glucose consumption was 96.75 %, 95.12 %, 94.85 %, 98.10 %, and 96.75 %. If the content was 10^{-6} M, the glucose consumption rate of HepG2 cells was the lowest. In comparison to the blank control group, the cells decreased by 3.25 %, 4.88 %, 5.15 %, 1.90 %, and 3.25 %, and the difference was significant ($P < 0.05$). Therefore, 10^{-6} M was selected as the optimal modeling concentration. In conclusion, high glucose and high insulin can induce IR in HepG2 cells.

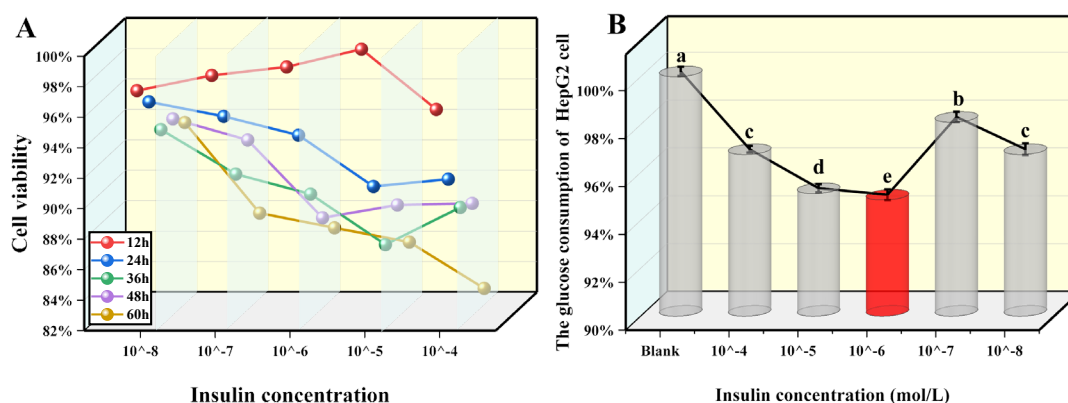


Fig 4. Screening of IR model condition. Blank is the standard HepG2 cell, without insulin and drug intervention. (A) Impact of various contents of insulin on HepG2 cell viability at different points. (B) Effect of insulin content on the glucose consumption of HepG2 cells under the optimal time. ($X \pm S$, $n=6$). Tukey's test: Different letters indicate significant differences ($p < 0.05$), the same letters indicate not significant differences.

Activity and glucose consumption of picoside I against IR-HepG2 cells were determined

Fig. 5(A) presents that the cell viability was more than 90 % after 24 h. However, when the concentration of picoside I was 80 $\mu\text{g/mL}$, the IR-HepG2 cell viability reached 98 %, which had the slightest effect compared with other concentrations. Therefore, 80 $\mu\text{g/mL}$ was selected as the optimal concentration of picoside I.

As shown in Fig. 5(B), compared with the glucose consumption of the negative group, IR-HepG2 cells glucose consumption treated with picoside I and the positive group was increased, increasing by 4.13 % and 1.72 %, respectively, and the difference was statistically significant ($P < 0.05$). Compared with the positive group, IR-HepG2 cell's glucose consumption significantly increased by 2.37 % after treatment with picoside I. This further proved that picoside I could improve glucose consumption and alleviate IR in IR-HepG2 cells.

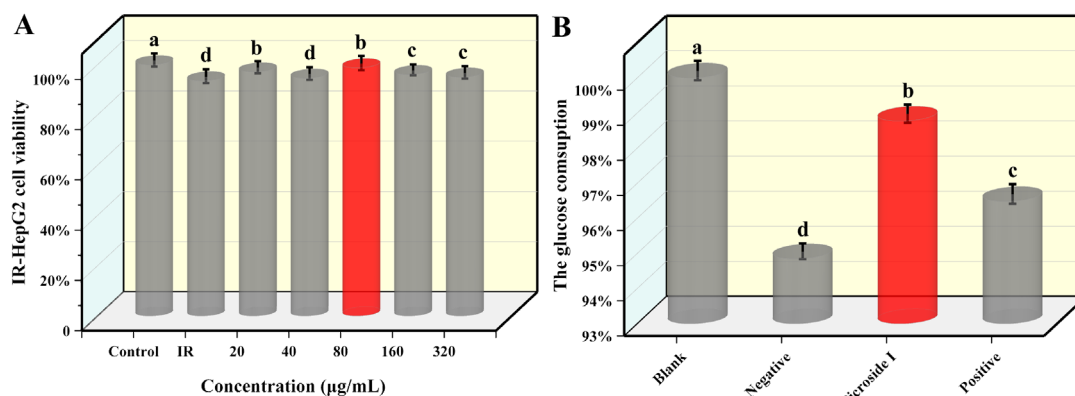


Fig 5. Determination of IR-HepG2 cells experimental. Blank is the standard HepG2 cell, without insulin and drug intervention. Negative is the IR-HepG2 cells without compound treatment. Picoside I is IR-HepG2 cells treated with rosiglitazone. Positive is positive group, IR-HepG2 cells treated with rosiglitazone. **(A)** Effect of picoside I on IR-HepG2 cell viability. **(B)** The glucose consumption of the IR-HepG2 cells by treating with 80 µg/mL picoside I. ($X \pm S$, $n=6$). Tukey's test: Different letters indicate significant differences ($p < 0.05$), the same letters indicate not significant differences.

Effects of picoside I on MDA content in IR-HepG2 cells

As shown in Fig. 6, the MDA content in the negative group exceeded that of the blank control group, and the difference was statistically obvious ($P < 0.05$), indicating that MDA content increased when IR occurred. After 24 h treatment with picoside I and positive control (rosiglitazone), compared with the negative group, the MDA content decreased significantly, decreased by 37.29% and 32.2%, respectively, and the difference was statistically significant ($P < 0.05$). The outcomes showed that picoside I might decrease MDA content in IR-HepG2 cells and reduce the oxidative stress state of cells.

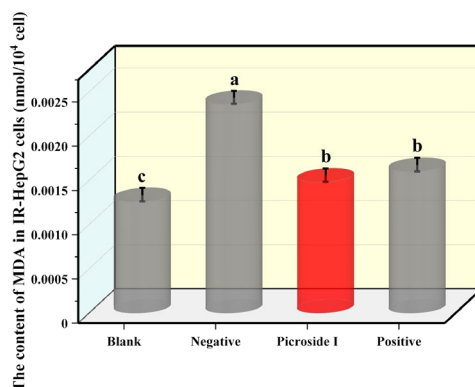


Fig 6. Effects of 80 µg/mL picoside I on MDA content of IR-HepG2 cell. Blank is the standard HepG2 cells, without insulin and drug intervention. Negative is the negative group, the IR-HepG2 cells without compound treatment. Positive is positive groups, IR-HepG2 cells treated with rosiglitazone. ($X \pm S$, $n=6$). Tukey's test: Different letters indicate significant differences ($p < 0.05$), the same letters indicate not significant differences.

Effects of picroside I on SOD activity of IR-HepG2 cells

Fig. 7 exhibited that the SOD activity in the negative group was significantly lower than that in the blank group, which decreased by 46.15 %, indicating that SOD activity was reduced in cells with IR. After adding picroside I into IR-HepG2 cells, the SOD activity was significantly increased, compared to that of the negative group and positive group. The difference was statistically obvious ($P < 0.05$). The outcomes show that picroside I might enhance the SOD activity and antioxidant capacity of IR-HepG2 cells.

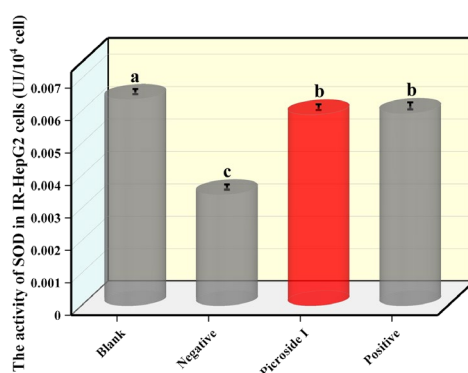


Fig 7. Effects of 80 $\mu\text{g/mL}$ picroside I on SOD activity of IR-HepG2 cells. Blank is the HepG2 cells without insulin and drug intervention. Negative is the IR-HepG2 cells without compound treatment. Positive is positive group, IR-HepG2 cells treated with rosiglitazone. ($\bar{X} \pm S$, $n=6$). Tukey's test: Different letters indicate significant differences ($p < 0.05$), the same letters indicate not significant differences.

Discussion and Conclusions

This research is significant for the creation of new drugs for T2DM derived from natural products. Unlike other studies, this study not only examined the antioxidant effects of picroside I by analyzing its scavenging capacity and overall reducing ability against $\text{DPPH}\cdot$, $\text{ABTS}\cdot^+$, and $\text{OH}\cdot$, but also looked at its impact on carbohydrate degradation and glucose absorption. This was achieved by testing its ability to inhibit α -glucosidase and α -amylase, thus examining the hypoglycemic effects of picroside I through multiple mechanisms. The results showed that picroside I displayed strong antioxidant properties, as well as strong inhibition in α -glucosidase and α -amylase, reducing the conversion of non-carbohydrate substances to glucose and displaying multi-pathway hypoglycemic activity. In the IR-HepG2 cell model, the addition of picroside I led to increased glucose consumption and decreased production of free radical metabolites, with IR decreasing as the concentration of the compound increased. This study investigated the effect of picroside I on oxidative stress and hypoglycemic activity at the cellular level, providing a theoretical foundation and experimental evidence for future experiments in animal models.

Acknowledgements

The research was supported by the Sichuan Science and Technology Support Program (Grant No. 19ZDYF0704); the Chunhui Project of the Ministry of Education of China (Grant No. Z2017059); and the Innovation Training Program for College Students (Grant No. 201710623011).

References

1. Biessels, G. J.; Gispen, W. H. *Neurobiol. Aging.* **2005**, 26 Suppl 1, 36-41. DOI: <http://dx.doi.org/10.1016/j.neurobiolaging.2005.08.015>
2. Whiting, D. R.; Guariguata, L.; Weil, C.; Shaw, J. *Diabetes Res. Clin. Prac.* **2011**, 94, 311-321. DOI: <http://dx.doi.org/10.1016/j.diabres.2011.10.029>
3. Fu, Z.; Gilbert, E. R.; Liu, D. *Curr. Diabetes Rev.* **2013**, 9, 25-53.
4. Brannmark, C.; Nyman, E.; Fagerholm, S.; Bergenholm, L.; Ekstrand, E.; Cedersund, G.; Stralfors, P. *J. Biol. Chem.* **2013**, 288, 9867-9880. DOI: <http://dx.doi.org/10.1074/jbc.M112.432062>
5. Tangvarasittichai, S. *World J. Diabetes.* **2015**, 6, 456-80. DOI: <http://dx.doi.org/10.4239/wjd.v6.i3.456>
6. Farrugia, G.; Balzan, R. *Fron. Oncol.* **2012**, 2, 64-64. DOI: <http://dx.doi.org/10.3389/fonc.2012.00064>
7. Cossarizza, A.; Ferraresi, R.; Troiano, L.; Roat, E.; Gibellini, L.; Bertocelli, L.; Nasi, M.; Pinti, M. *Nat. Protoc.* **2009**, 4, 1790-1797. DOI: <http://dx.doi.org/10.1038/nprot.2009.189>
8. Siddique, Y. H.; Ara, G.; Afzal, M. *Dose-Response.* **2012**, 10, 1-10. DOI: <http://dx.doi.org/10.2203/dose-response.10-002.Siddique>
9. Fernandes, A. C. F.; Melo, J. B.; Genova, V. M.; Santana, A. L.; Macedo, G. *Recent Pat. Food, Nutr. Agric.* **2022**, 13, 3-16. DOI: <http://dx.doi.org/10.2174/2212798412666210528130001>
10. Imam, M. U.; Musa, S. N. A.; Azmi, N. H.; Ismail, M. *Int. J. Mol. Sci.* **2012**, 13, 12952-12969. DOI: <http://dx.doi.org/10.3390/ijms131012952>
11. Sung, M.; Park, S. S.; Kim, S.; Han, C.; Hur, J. *Food Sci. Biotechnol.* **2014**, 23, 1615-1621. DOI: <http://dx.doi.org/10.1007/s10068-014-0220-3>
12. Balkan, B. M.; Kismali, G.; Alpay, M.; Sayiner, S.; Turan, D.; Balkan, A. B.; Salmanoglu, B.; Karagul, H.; Sel, T. *Kafkas Universitesi Veteriner Fakultesi Dergisi.* **2016**, 22, 865-869. DOI: <http://dx.doi.org/10.9775/kvfd.2016.15499>
13. Chen, W.; Shaw, L.; Chang, P.; Tung, S.; Chang, T.; Shen, C.; Hsieh, Y.; Wei, K. *Experimental and Therapeutic Medicines.* **2016**, 11, 1231-1238. DOI: <http://dx.doi.org/10.3892/etm.2016.3077>
14. Sriset, Y.; Chatuphonprasert, W.; Jarukamjorn, K. *Tropical J. Pharm. Res.* 2019, 18, 1001-1007. DOI: <http://dx.doi.org/10.4314/tjpr.v18i5.13>
15. Lee, H.; Lim, Y. *J. Nutr. Biochem.* **2018**, 57, 77-85. DOI: <http://dx.doi.org/10.1016/j.jnutbio.2018.03.016>
16. Polce, S. A.; Burke, C.; Franca, L. M.; Kramer, B.; de Andrade Paes, A. M.; Carrillo-Sepulveda, M. A. *Nutrients.* **2018**, 10. DOI: <http://dx.doi.org/10.3390/nu10050531>
17. Balabolkin, M. L.; Klebanova, E. M. *Terapevticheskii.* 2003, 75, 72-77.
18. Taylor, R. *Journal of the Royal College of Physicians of Edinburgh.* **2017**, 47, 168-171. DOI: <http://dx.doi.org/10.4997/JRCPE.2017.216>
19. Li, C.; He, J.; Zhou, X.; Xu, X. *China Journal of Chinese Materia Medica.* **2017**, 42, 2254-2260. DOI: <http://dx.doi.org/10.19540/j.cnki.cjcmm.20170307.014>
20. Schmidt, M. I.; Bracco, P. A.; Duncan, B. B. *Lancet Diabetes Endocrinol.* **2019**, 7, 424. DOI: [http://dx.doi.org/10.1016/S2213-8587\(19\)30148-2](http://dx.doi.org/10.1016/S2213-8587(19)30148-2)
21. Jamal, P.; Barkat, A. A.; Amid, A. *Afr. J. Biotechnol.* **2011**, 10, 18788-18794. DOI: <http://dx.doi.org/10.5897/AJB11.2754>

22. Han, H.; Li, Z.; Gao, Z.; Yin, X.; Dong, P.; Yang, B.; Kuang, H. *Nat. Prod. Res.* **2019**, *33*, 2845-2850. DOI: <http://dx.doi.org/10.1080/14786419.2018.1508143>
23. Chen, W.; Shen, Y.; Su, H.; Zheng, X. *Chem.-Biol. Interact.* **2014**, *219*, 83-89. DOI: <http://dx.doi.org/10.1016/j.cbi.2014.05.010>
24. Floegel, A.; Kim, D.; Chung, S.; Koo, S. I.; Chun, O. K. *J. Food Compos. Anal.* **2011**, *24*, 1043-1048. DOI: <http://dx.doi.org/10.1016/j.jfca.2011.01.008>
25. Chi, C.; Hu, F.; Wang, B.; Li, T.; Ding, G. *J. Funct. Foods.* **2015**, *15*, 301-313 DOI: <http://dx.doi.org/10.1016/j.jff.2015.03.045>
26. Vijayalakshmi, M.; Ruckmani, K. *Bangladesh Journal of Pharmacology.* **2016**, *11*, 570-572. DOI: <http://dx.doi.org/10.3329/bjp.v11i3.27663>
27. Yilmazer-Musa, M.; Griffith, A. M.; Michels, A. J.; Schneider, E.; Frei, B. *J. Agric. Food Chem.* **2012**, *60*, 8924-8929. DOI: <http://dx.doi.org/10.1021/jf301147n>
28. Kazeem, M. I.; Adamson, J. O.; Ogunwande, I. A. *BioMed Research International.* **2013**, 2013. DOI: <http://dx.doi.org/10.1155/2013/527570>